CO_2 Capture

International Edition: DOI: 10.1002/anie.201507846
German Edition: DOI: 10.1002/ange.201507846

Capture CO_2 from Ambient Air Using Nanoconfined Ion Hydration

*Xiaoyang Shi, Hang Xiao, Klaus S. Lackner, and Xi Chen**

Abstract: *Water confined in nanoscopic pores is essential in determining the energetics of many physical and chemical systems. Herein, we report a recently discovered unconventional, reversible chemical reaction driven by water quantities in nanopores. The reduction of the number of water molecules present in the pore space promotes the hydrolysis of* CO_3^{2-} *to* HCO_3^- *and* OH^-*. This phenomenon led to a nano-structured* CO_2 *sorbent that binds* CO_2 *spontaneously in ambient air when the surrounding is dry, while releasing it when exposed to moisture. The underlying mechanism is elucidated theoretically by computational modeling and verified by experiments. The free energy of* CO_3^{2-} *hydrolysis in nanopores reduces with a decrease of water availability. This promotes the formation of* OH^-*, which has a high affinity to* CO_2*. The effect is not limited to carbonate/bicarbonate, but is extendable to a series of ions. Humidity-driven sorption opens a new approach to gas separation technology.*

Ion hydration and dehydration at interfaces play a key role in a plethora of chemical,[1,2] physical,[3] biological,[4] and environmental systems.[5] Owing to the hydration water at the interface, the rate and extent of various types of chemical reactions may be significantly enhanced.[6–11] The hydration of ions does not only affect the physical structure and dynamics of water molecules,[12] but also the chemical energy transfer through the formation of highly structured water complexes.[13,14] Indeed, ion hydration could promote the energy level of water structures, which may receive wide applications such as in energy storage with anhydrous salts,[15] enhancement of the free energy of binding ligands to biological systems,[16] and gas separation using modified basicity of ionic sorbent.[17]

Previous experimental observations provided detailed structural information and information on the dissociation of interfacial hydration water at the molecular level.[11,18] Molecular modeling has contributed significantly to a better understanding and interpretation of the observed hydration phenomena of ions, ion pairs, and solid–liquid interfaces, such as evaluating ion hydration free energy,[19] analyzing water density at solid hydrophobic surfaces,[20] as well as understanding hydration energy and structural changes with reduced water activity,[21,22] which showed a high degree of positional ordering parallel to the surface. Many more contemporary issues, such as storage in both water and energy, and climate change, require a better understanding of the structure and dynamics of ion hydration on solid surfaces.[23,24]

Of particular interest in this study is a mechanism for capturing CO_2 directly from ambient air with a sorbent swing that is driven by a humidity swing involving ion hydration/dehydration in an ion exchange resin.[25–27] The urgency of the development of CO_2 capture from ambient air is discussed elsewhere.[28] The regeneration of the sorbent simply uses inexpensive water. Evaporation in ambient air drives the sorbent to absorb CO_2 as it dries, and hydration releases CO_2 when wet. While the effect has been well documented, it so far lacks a simple explanation. We therefore sought to elucidate the underlying mechanism and verify it by nanomaterials. Interfacial water has been speculated to play two important roles: it may provide a medium for reactions, and may protonate reactants through water dissociation.

CO_2 absorption and desorption on a nanoporous material with CO_3^{2-} as the mobile anion at low humidity could be depicted as the reactions of water dissociation and formation of bicarbonate and hydroxide ions, as shown in [Equations (1–4)] and Figure 1.

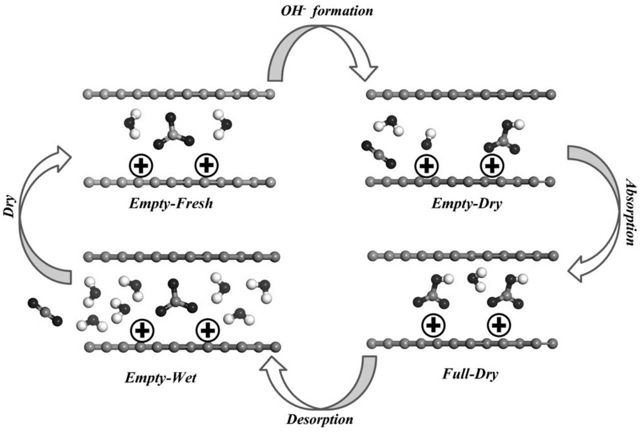

Figure 1. Reaction pathway of CO_2 absorption/desorption on nanostructural absorbent. The Empty–Fresh state is the sorbent in dry condition with a few water molecules in the surrounding. The Empty–Dry state is when H_2O splits into H^+ ion and OH^- ion which are ready to absorb CO_2, and H^+ ion is combined with CO_3^{2-} forming HCO_3^- ion [Eqs. (1) and (2)]. The Full–Dry state is the fully loaded sorbent in the dry condition [Eq. (3)]. Equations (1–3) present the absorption process. The Empty–Wet state is the regenerating absorbent releases CO_2 in the wet condition (desorption [Eq. (4)]).

---

[*] X. Y. Shi, H. Xiao, Prof. X. Chen
Department of Earth and Environmental Engineering
Columbia University
905E Mudd, 500 West 120th Street
New York, NY 10027 (USA)
E-mail: xichen@columbia.edu

Prof. K. S. Lackner
School of Sustainable Engineering & Built Environment
Arizona State University
Tempe, AZ 85287-9309 (USA)

Supporting information for this article can be found under:
http://dx.doi.org/10.1002/anie.201507846.

$$H_2O \Leftrightarrow H^+ + OH^- \quad (1)$$

$$CO_3^{2-} + H^+ \Leftrightarrow HCO_3^- \quad (2)$$

$$OH^- + CO_2 \Leftrightarrow HCO_3^- \quad (3)$$

$$HCO_3^- + HCO_3^- \Leftrightarrow CO_3^{2-} + CO_2 + H_2O \quad (4)$$

The activity of water in the nanopores governs the all of the ion interactions on the absorbent. Here, we postulated that the reduction in water activity results in a loss of stability of the carbonate ion, which will be replaced by a hydroxide and a bicarbonate ion:

$$CO_3^{2-} + n\,H_2O \Leftrightarrow HCO_3^- + OH^- + (n-1)\,H_2O \quad (5)$$

The material is a stronger CO_2 sorbent in dry conditions (n is small) with the help of more OH^- ions than in wet conditions (n is large). As n decreases, the equilibrium in [Eq. (5)] shifts to the right, which seems to go against the mass action law. However, the $(n-1)$ water molecules on the right of the equation are not simple bystanders but participate in the reaction through hydration. The reduction in water activity inside a nano-structured pore is also far more dramatic than what can be achieved in aqueous solutions. For example, inside the nanostructured pore the ratio of CO_3^{2-} ions and H_2O may be as high as 1:1 (as verified by following experiments), instead of 1:20 in a saturated Na_2CO_3 solution at 20 °C. This allows for a significant driving force for this change in equilibrium owing to changes in the size of the ion hydration clouds. The total equation taking into account hydration water is represented by [Eq. (6)].

$$\begin{aligned} CO_3^{2-}\cdot n\,H_2O \Leftrightarrow {} & HCO_3^-\cdot m_1\,H_2O + \\ & OH^-\cdot m_2\,H_2O + (n-m_1-m_2-1)\,H_2O \end{aligned} \quad (6)$$

The chemical reaction shifts to the right hand side with a small number of water molecules to produce more OH^- ions, which is beneficial for CO_2 absorption, and it swings to the left hand side with a large number of water molecules present.

During the desorption stage, [Eq. (4)], the partial pressure of CO_2 over a wet, fully-loaded bicarbonate state sorbent is comparable to the equilibrium partial pressures over a one-molar sodium bicarbonate solution. At 25 °C, the equilibrium partial pressure of CO_2 above a one molar $NaHCO_3$ solution is 6.0 kPa when 20% of the HCO_3^- is decomposed to CO_3^{2-}.[29] This suggests that the unusual state is not the wet state (that is, the reaction [Eq. (4)] is spontaneously releasing CO_2 in the wet state), but the dry absorption state in the CO_2 capture system.

We postulated that the energetically favorable state of this system [Eq. (6)] can be shifted with the number of water molecules available for hydration. This hypothesis will be verified using molecular simulations. A methodology combining Molecular Dynamics (MD) and Quantum Mechanics (QM) is outlined in Figure 2. It can calculate energy states in a hypothetical cycle connecting aqueous states to ionic states in the vacuum. In the corresponding thermodynamic cycle of the proposed process, a sequence of states is considered. The objective is to quantify the total free energy ΔG^0 of [Eq. (6)] as the number of surrounding water molecules (n) changes.

$$\begin{tikzcd}
2Na^+, CO_3^{2-}, nH_2O \arrow[r, "\Delta G^0"] \arrow[d, "\Delta G_1^0"'] & 2Na^+, HCO_3^-, OH^-, (n-1)H_2O \\
2Na^+, CO_3^{2-}, H_2O \arrow[r, "\Delta G_3^0"'] & 2Na^+, HCO_3^-, OH^- \arrow[u, "\Delta G_2^0"']
\end{tikzcd}$$

$$\Delta G^0 = \Delta G_1^0 + \Delta G_2^0 + \Delta G_3^0$$

Figure 2. Thermodynamic cycle for calculating reaction energy change with water numbers. $\Delta G_1{}^0$ and $\Delta G_2{}^0$ denote the hydration standard-state Gibbs free energy changes of system 1 (S1, two Na^+, one CO_3^{2-} hydration) and system 2 (S2, two Na^+, one HCO_3^- and with one OH^- hydration), respectively. $\Delta G_3{}^0$ represents the standard-state Gibbs free energy change of the reaction $Na_2CO_3 + H_2O \Leftrightarrow NaHCO_3 + NaOH$ in vacuum at room temperature. The total free energy ΔG can be obtained as $\Delta G^0 = \Delta G_1{}^0 + \Delta G_2{}^0 + \Delta G_3{}^0$. Using MD simulations of relevant systems, free energies $\Delta G_1{}^0$ and $\Delta G_2{}^0$ can be determined by Thermodynamic Integration (TI); $\Delta G_3{}^0$ can be deduced from QM density functional theory (DFT). Two mobile cations (Na^+) were put into the system, in order to balance the anionic charges.

The free energy change for different numbers of water molecules present is calculated. The hydration free energies of S1 and S2 in the presence of water were plotted against the water numbers (n; Figure 3 A). The two systems have a one-to-one correspondence, since one water molecule reacts with one carbonate ion to form a bicarbonate and a hydroxide ion. The region around each ion dissolved in water can be divided into two parts: a hydration shell, in which the water is immobilized and electrostricted, and bulk water, which is still attracted by the Coulomb electric field of the ion, but where the water is mobile and not bound to the ion. Based on the MD modeling results, typically the free energies of hydration in the $Na^+{-}CO_3^{2-}{-}H_2O$ system and in the $Na^+{-}HCO_3^-{-}OH^-$ system decrease, that is, binds more strongly, when the number of water molecules increases from 0 to 40. These hydration free energies are stable in the range of 40 to 60 water molecules. The free energy $\Delta G_1{}^0$ fluctuates rapidly with the small number of water molecules available. We speculate that this reflects the filling of an inner hydration shell, where different number of water molecules would result in different geometries. If more water is available, the Coulomb potential of the ion likely causes a gradual decrease in the free energy until the system asymptotically reaches a state similar to that in free water. If the water molecules are more than 300, the hydration free energies of S1 and S2 stabilize around $-80\ \mathrm{kcal\,mol^{-1}}$ and $-50\ \mathrm{kcal\,mol^{-1}}$, respectively (Supporting Information, Figure S1).

In Figure 3B, attention is restricted to the free energy change ΔG^0 of reaction pathway [Eq. (6)]. According to Figure 2, $\Delta G^0 = \Delta G_1{}^0 + \Delta G_2{}^0 + \Delta G_3{}^0$, where $\Delta G_3{}^0 = -14.63\ \mathrm{kcal\,mol^{-1}}$ is the reaction energy of $Na_2CO_3 + H_2O \Leftrightarrow NaHCO_3 + NaOH$ in vacuum at room temperature. The free energy changes based on the above MD and QM free

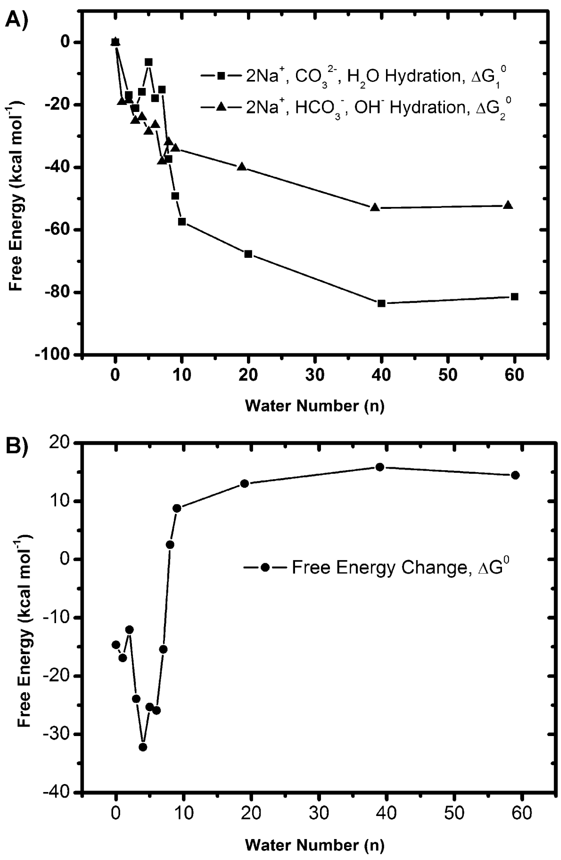

Figure 3. Free Energy Change. A) Hydration free energy change with water numbers. In the carbonate ion system simulations (S1) ΔG_1^0, the CO_3^{2-}: H_2O ratio is selected to be 1:1, 1:2, 1:3, 1:4, 1:5, 1:6, 1:7, 1:8, 1:9, 1:10, 1:20, 1:40, and 1:60, respectively, shown as rectangular points. For the bicarbonate ion system (S2) ΔG_2^0, the HCO_3^- to H_2O ratio is tested at 1:0, 1:1, 1:2, 1:3, 1:4, 1:5, 1:6, 1:7, 1:8, 1:9, 1:19, 1:39, and 1:59, respectively, shown as triangle points, from dense to dilute solution. B) Equation (6) reaction free energy change with water numbers. Circle points are the total free energy change ΔG^0 of reaction pathway, plotted as a function of the number of water molecules.

energy calculations are shown in Figure 3B. The circle points show the free energy is negative when there are less than 7 water molecules, favoring the formation of hydroxide ions. With the increase in the number of water molecules from 8 to 60, the free energy difference increases rapidly from negative to positive value, then becomes stable at a plateau of 15 $kcal\,mol^{-1}$ in bulk water. The experimental value of the carbonate hydrolysis equilibrium constant K in bulk aqueous solution is 1.9×10^{-4}, the free energy of hydrolysis is 5.08 $kcal\,mol^{-1}$.[30] The present analysis showed, at least in terms of qualitative trends, that the equilibrium between carbonate and bicarbonate ions in an aqueous solution inside nanostructured pores is affected by the number of water molecules present. With the reduction of the number of ambient water molecules, it becomes energetically favorable to form hydrated bicarbonate and hydroxide ions, whereas carbonate ion hydration occurs in wet conditions. In a relatively dry environment, the amount of water bound to the absorbent is small and a large amount of hydroxide ions exist, which promotes the absorption of CO_2, while the desorption process is favored in a wet environment, which explains the moisture swing used for direct air capture.[25]

To confirm the effect of water on a CO_2 capture sorbent, we performed a CO_2 absorption experiment using activated carbon powder soaked in Na_2CO_3 solution which has a high ratio of isolated carbonate ion to water molecules in the nanopores. An experimental device (Supporting Information, Figure S2) with temperature and humidity control was set up to determine the CO_2 absorption/desorption performance.

The curve of CO_2 concentration changes with relative humidity is shown in Figure 4A. It shows that activated carbon impregnated with carbonate ions has a very pronounced moisture effect on CO_2 absorption. The CO_2 absorption process took place when the dew point was decreasing from 23.0 °C to −2.0 °C. In this process, relatively larger amounts of OH^- ions were produced which could react with CO_2 in the gas phase without a free energy barrier.[31] In contrast, if the sorbent is exposed to higher level of moisture, the concentration of CO_2 equilibrated in the air is at a relatively high level because of low hydroxide ion concentration on the sorbent. The 420 ppm lowest CO_2 concentration at the local vicinity is because the nanopores physically constrains a relatively small amount of CO_2, and subsequently

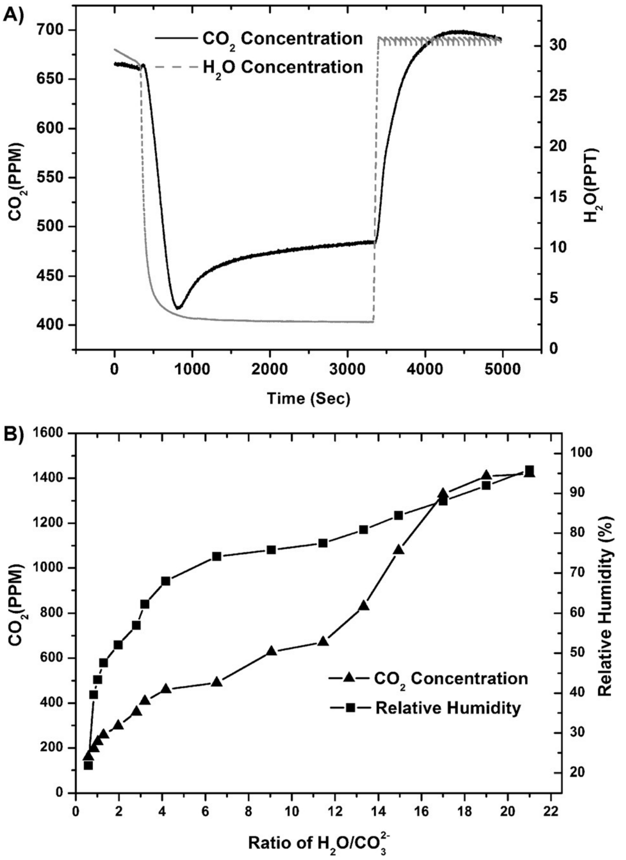

Figure 4. Experimental verification. A) CO_2 concentration changes with relative humidity. Black solid line is the CO_2 concentration. Grey dash line is the Dew Point in the experimental device. B) CO_2 equilibrium concentration and relative humidity correspond to the water to carbonate ions ratio. The rectangular points show the H_2O to CO_3^{2-} ion ratio change with RH change. The triangular points show CO_2 equilibrium concentration change with H_2O to CO_3^{2-} ion ratio change.

releases a part of CO_2 to achieve the equilibrium partial pressure of CO_2 over the sorbent. The effect of activated carbon without Na_2CO_3 on CO_2 absorption was also measured as a reference test. The dew point was also decreasing from 23.0°C to −2.0°C, and then increasing back to 23.0°C. The CO_2 concentration decreases from 655 ppm to 639 ppm then back to 655 ppm, only with 20 ppm amplitude variation. It confirms that the factor of CO_3^{2-} ions with different number of water molecules plays a decisive role in CO_2 absorption.

Another experiment was conducted using the same sample as above. The same experimental device (Figure S2) was employed to determine the sample weights and CO_2 equilibrium concentrations at different humidity conditions (Figure 4B). First, the weight of absorbent sample at each dew point was measured in the CO_2 free condition. The weight change of the sample is due to the changing amount of water adsorbed on the surface of activated carbon under different humidity conditions. Then, the ratio of water molecules to CO_3^{2-} ions can be calculated by the weight change. Rectangular points show the H_2O to CO_3^{2-} ion ratio increases with RH increases. Then, with the known ratio of water molecules to CO_3^{2-} ions at each RH point, the CO_2 equilibrium concentration was recorded under the each same RH point in the experimental device (Figure S2). The equilibrium concentration of CO_2 increases as the ratio of H_2O to CO_3^{2-} ion increases (Figure 4B). The experiment validated the theoretical results (Figure 3B). In drier conditions, a lower ratio of H_2O to CO_3^{2-} ion ratio is conducive to produce larger amounts of OH^- ions to absorb CO_2.

We demonstrated an unconventional chemical reaction in nano-confinement and applied it to capture of CO_2 driven by inexpensive water. This mechanism sheds light on a vast number of chemical processes in the nano-environment, such as interactions between water and a series of basic or acidic ions. The finding has wide potential applications, including on designs for more efficient energy-saving absorbents.

Experimental Section

The CO_2 absorption sorbent sample 0.0395 g was made by soaking the activated carbon into a 1M solution of sodium carbonate for four hours, then it was dried in ambient air. Dry sorbent was put into the sample chamber, in which the air humidity dew point was set to 23.0°C (28 parts/thousand) first and then turned down to −2.0°C (2.5 parts/thousand) to detect the variation of CO_2.

The second experiment was conducted by using 0.204 g activated carbon with 0.2 mL 1M Na_2CO_3 solution dripped on it, then the sample was dried in vacuum chamber for 72 hours. Next, the sorbent was fully loaded with CO_2 under the surrounding of dry (Dew Point is −10°C) and 400 ppm CO_2 atmosphere.

Acknowledgements

We thank Tao Wang and Allen Wright for help with some experiments. We, and especially K.S.L., would like to thank and acknowledge Agustin J. Colussi for stimulating discussions and excellent advice and suggestions that greatly encouraged us in the pursuit of this research.

Keywords: air–water interfaces · CO_2 capture · free energy · ion hydration · molecular dynamics

How to cite: *Angew. Chem. Int. Ed.* **2016**, *55*, 4026–4029
Angew. Chem. **2016**, *128*, 4094–4097

---

[1] H. Mishra, S. Enami, R. J. Nielsen, L. A. Stewart, M. R. Hoffmann, W. A. Goddard, A. J. Colussi, *Proc. Natl. Acad. Sci. USA* **2012**, *109*, 18679.
[2] W. Kunz, J. Henle, B. W. Ninham, *Curr. Opin. Colloid Interface Sci.* **2004**, *9*, 19.
[3] B. Hribar, N. T. Southall, V. Vlachy, K. A. Dill, *J. Am. Chem. Soc.* **2002**, *124*, 12302.
[4] P. J. Steinbach, B. R. Brooks, *Proc. Natl. Acad. Sci. USA* **1993**, *90*, 9135.
[5] C. Caleman, J. S. Hub, P. J. van Maaren, D. van der Spoel, *Proc. Natl. Acad. Sci. USA* **2011**, *108*, 6838.
[6] N. Shapiro, A. Vigalok, *Angew. Chem. Int. Ed.* **2008**, *47*, 2849; *Angew. Chem.* **2008**, *120*, 2891.
[7] J. Israelachvili, H. Wennerstrom, *Nature* **1996**, *379*, 219.
[8] D. Chandler, *Nature* **2005**, *437*, 640.
[9] A. Verdaguer, G. M. Sacha, H. Bluhm, M. Salmeron, *Chem. Rev.* **2006**, *106*, 1478.
[10] S. Enami, M. R. Hoffmann, A. J. Colussi, *J. Phys. Chem. Lett.* **2010**, *1*, 1599.
[11] S. Enami, L. A. Stewart, M. R. Hoffmann, A. J. Colussi, *J. Phys. Chem. Lett.* **2010**, *1*, 3488.
[12] P. Jungwirth, D. J. Tobias, *Chem. Rev.* **2006**, *106*, 1259.
[13] Z. S. Zidi, *J. Chem. Phys.* **2005**, *123*, 064309.
[14] Z. Zhao, D. M. Rogers, T. L. Beck, *J. Chem. Phys.* **2010**, *132*, 014502.
[15] M. Ghommem, G. Balasubramanian, M. R. Hajj, W. P. Wong, J. A. Tomlin, I. K. Puri, *Int. J. Heat Mass Transfer* **2011**, *54*, 4856.
[16] D. Hamelberg, J. A. McCammon, *J. Am. Chem. Soc.* **2004**, *126*, 7683.
[17] K. J. Fricker, A.-H. A. Park, *Chem. Eng. Sci.* **2013**, *100*, 332.
[18] C. S. Tian, Y. R. Shen, *Proc. Natl. Acad. Sci. USA* **2009**, *106*, 15148.
[19] D. J. Giesen, G. D. Hawkins, D. A. Liotard, C. J. Cramer, D. G. Truhlar, *Theor. Chem. Acc.* **1997**, *98*, 85.
[20] A. J. Patel, P. Varilly, D. Chandler, *J. Phys. Chem. B* **2010**, *114*, 1632.
[21] J. Wang, A. G. Kalinichev, R. J. Kirkpatrick, *Geochim. Cosmochim. Acta* **2006**, *70*, 562.
[22] J. Wang, A. G. Kalinichev, R. J. Kirkpatrick, *J. Phys. Chem. C* **2009**, *113*, 11077.
[23] J. Carrasco, A. Hodgson, A. Michaelides, *Nat. Mater.* **2012**, *11*, 667.
[24] K. J. Tielrooij, N. Garcia-Araez, M. Bonn, H. J. Bakker, *Science* **2010**, *328*, 1006.
[25] K. S. Lackner, *Eur. Phys. J. Spec. Top.* **2009**, *176*, 93.
[26] T. Wang, K. S. Lackner, A. Wright, *Environ. Sci. Technol.* **2011**, *45*, 6670.
[27] T. Wang, K. S. Lackner, A. B. Wright, *Phys. Chem. Chem. Phys.* **2013**, *15*, 504.
[28] K. S. Lackner, S. Brennan, J. M. Matter, A.-H. A. Park, A. Wright, B. van der Zwaan, *Proc. Natl. Acad. Sci. USA* **2012**, *109*, 13156.
[29] C. R. Harte, E. M. Baker, *Ind. Eng. Chem.* **1933**, *25*, 1128.
[30] F. C. Frary, A. H. Nietz, *J. Am. Chem. Soc.* **1915**, *37*, 2268.
[31] Z. Peng, K. M. Merz, *J. Am. Chem. Soc.* **1993**, *115*, 9640.

Received: August 21, 2015
Revised: February 1, 2016